Protein Anatomy: C-Tail Region of Human Tau Protein as a Crucial Structural Element in Alzheimer's Paired Helical Filament Formation *in Vitro*

Hiroshi Yanagawa,*,‡ Sang-Ho Chung,‡,§ Yoko Ogawa,‡ Kazuki Sato,‡ Teiko Shibata-Seki,|| Junji Masai,|| and Koichi Ishiguro‡

Mitsubishi Kasei Institute of Life Sciences, 11 Minamiooya, Machida, Tokyo 194, Japan, and Yokohama Research Center, Mitsubishi Chemical Corporation, 1000 Kamoshida, Aoba-ku, Yokohama 227, Japan

Received September 30, 1997; Revised Manuscript Received December 11, 1997

ABSTRACT: Tau is a microtubule-associated protein in mammalian brain. In Alzheimer's disease, this protein is present in the somatodendritic compartment of certain nerve cells, where it forms a portion of paired helical filament, the major constituent of the neurofibrillary tangle. For clarification of the mechanism of this formation, recombinant human tau and its fragments (N-terminal half, C-terminal half, and 4-repeats) expressed in *Escherichia coli* were prepared, eight peptide fragments (C-tails 1−8) of the C-tail region were synthesized, and the conformation and capacity for aggregation essential for filamentous structure formation *in vitro* were examined. Recombinant full-length tau, the N-terminal half, 4-repeats, and the C-terminal half did not form filamentous structures in aqueous solution after standing at 20 °C. Peptides corresponding to the C-tail region of tau, C-tail 5, C-tail 7, and C-tail 8, produced the paired filament or single straight filament in acidic solution. The rate of filament formation by each peptide was followed by circular dichroism, which showed the C-tails to have predominantly random coil structures immediately following dissolution in aqueous solution and be gradually converted to the β-sheet structure. The kinetics of aggregation were characterized by a delay period during which the solution remained clear, followed by a nucleation event which led to a growth phase, whose negative peak intensity at 218 nm in circular dichroism increased due to filamentous structure formation. This delay was eliminated by seeding supersaturated solution of preformed filaments. C-tails interacted with recombinant full-length tau to form definite single straight filament. The C-tail region of tau is thus shown indispensable to the formation of paired helical filament and nucleation to reduce the rate of paired helical filament formation in amyloidogenesis *in vitro*. These findings may provide some clarification of the pathogenesis of Alzheimer's disease.

The microtubule-associated protein tau has been isolated by copurification with tubulin from cells of many different species (*1, 2*), and its presence has been shown restricted almost entirely to axons in the brain (*3*−*5*). Tau promotes microtubule assembly and stability in the nervous system (*6*). Multiple isoforms of tau (six types) are generated from a single gene through alternative RNA splicing (*7*−*9*). In normal cells, this protein is associated with axonal microtubules, whereas in Alzheimer's disease, it is present in the somatodendritic compartment of certain nerve cells as the major component of the paired helical filament (PHF),[1] the principal constituent of the neurofibrillary tangle (*7, 10*). Its amount in Alzheimer's disease brain is about 8 times that in control cases (*11*), and the 3- and 4-repeat regions of tau isoforms are incorporated into the Pronase-resistant core of PHF (*12*). Current Alzheimer's disease research is conducted primarily to determine the nature of PHF deposits in the brain, and mechanisms leading to PHF formation, though partially understood, should be clarified more fully. To clarify the functions of tau under normal and pathological conditions, the structure and self-assembly of this protein should be examined (*13*−*19*). Recombinant human tau isoforms expressed in *Escherichia coli* have been shown biologically functional in microtubule assembly (*20*). The mechanism for PHF formation *in vivo* is not fully understood. Wille et al. showed Alzheimer-like PHFs to be formed from the recombinant constructs corresponding roughly to the C-terminal repeat region of tau but not from full-length recombinant tau isoforms (*19*). Caputo et al. noted many PHF-like fibrils to form from a synthetic peptide corresponding to C-terminal residues, 676−695, of βAPP in the presence of tau (*21*), suggesting the C-terminal fragment of βAPP to possibly be essential along with tau to PHF formation. Crowther et al. observed PHF-like filaments to be produced from a fragment of protein corresponding to 3-repeats under certain conditions (*22*). For clarification of

* To whom all correspondence should be addressed. Telephone: 427-24-6293. Fax: 427-24-6317.

‡ Mitsubishi Kasei Institute of Life Sciences.

§ Present address: Department of Microbiology, Mokwon University, Taejon 301-729, Korea.

|| Mitsubishi Chemical Corp.

[1] Abbreviations: PHF(s), paired helical filament(s); SSF(s), single straight filament(s); βAPP, β amyloid precursor protein; SDS, sodium dodecyl sulfate; PAGE, polyacrylamide gel electrophoresis; IPTG, isopropyl 1-thio-β-D-galactoside; FAB, fast atom bombardment; AFM, atomic force microscopy; CD, circular dichroism; TFE, trifluoroethanol; MES, 2-morpholinoethanesulfonic acid; Aβ, β amyloid protein; PrP^{Sc}, scrapie prion protein; PrP^{C}, cellular prion protein; *H*, content of hydrophobic amino acids; *P*, content of charged amino acids.

S0006-2960(97)02426-4 CCC: $15.00
Published on Web 01/30/1998

the fine structure of tau, recombinant human tau and its fragments expressed in *E. coli* were prepared, and C-tail peptide fragments were synthesized to determine the particular portion of tau that is critically required for PHF formation.

MATERIALS AND METHODS

Amplification of Human Tau cDNA by PCR. Human brain cDNA library (cloned in λZAPII) was kindly provided by Prof. Sakaki (University of Tokyo, Japan). Phage was propagated in *E. coli* LE392 as the host cell. Phage DNA was prepared according to the plate lysate method (*23*), digested with the restriction enzyme *Eco*RI, and used as the template for PCR. To amplify full-length human tau cDNA, forward primer 1 (40-mer) containing oligonucleotide sequences comprised of the start codon ATG and its flanking region, 5′-TGTCGACTATCAGGTGAACTTTGAACCAG-GATGGCTGAGC-3′, and reverse primer 2 (40-mer) containing oligonucleotide sequences comprised of a complementary stop codon, TCA, and its flanking region, 5′-TTATTGACCGCCCCAGGGGCCTGATCA CAAACCCTG-CTTG-3′, were synthesized. The sequences of these primers were determined based on previously published human tau cDNA (*8*). PCR reactions with vent DNA polymerase (New England Biolabs) were conducted using standard buffer. The reaction mixture (100 μL) contained 1 μM of each primer, 200 μM of each dNTP, 200 ng of DNA template, 10 μL of 10 × PCR buffer, and 1−2 units of DNA polymerase. The best conditions for three-step PCR were template denaturation at 94 °C for 4 min followed by 30 cycles of 57 °C, 1 min; 73 °C, 2 min; 94 °C, 1 min, followed by a final cycle of 57 °C, 1 min; and 73 °C, 10 min.

Following confirmation of the above amplified whole sequence as true human tau cDNA (htau 24 isoform, 383 amino acids), the DNA was used as template DNA for preparation of the N-terminal half (lMet to 191Pro), C-terminal half (192Met to 383Leu), and 4-repeat (192Met to 318Leu) sequences of human tau cDNA through PCR amplification. The synthesized forward and reverse primers (40-mer) contained a *Nde*I site in the initiation condon, ATG, and a *Bam*HI site just behind the stop codon, respectively.

Cloning of PCR Products of Full-Length Tau in E. coli. Full-length PCR products were purified and their 5′ ends phosphorylated by T4 polynucleotide kinase. Plasmid DNA (pUC18) was digested with *Sma*I and dephosphorylated by calf intestinal alkaline phosphatase. *E. coli* cells (JM 109) were transformed with a ligation mixture, and the transformants containing the recombinant plasmid, pSC7, were selected as white colonies on the LB/X-gal plate containing ampicillin.

DNA Sequencing. Both strands of cloned human tau cDNA were sequenced by the dideoxy chain termination method (*24*) using a sequencing kit (United States Biochemical) with synthetic oligonucleotides as primers.

Construction of Expression Vectors. The plasmid pSC7 containing a full-length human tau cDNA insert was first modified to produce pSC71 possessing a unique *Nde*I restriction enzyme site in the initiation codon ATG, using two annealed oligonucleotides. To express cloned human tau cDNA in an *E. coli* pAR (*25*), a vector system was established. Following cleavage with *Nde*I/*Bam*HI of pSC71, the tau cDNA fragment thus obtained was subcloned into *Nde*I/*Bam*HI-cut plasmid pAR3040 to generate pSC15 whose human tau proteins can be synthesized under the control of T7 RNA polymerase promoter. The recombinant plasmid, pSC15, was transformed to *E. coli* BL21(DE3) cells. The recombinant plasmids, pSC17 (containing N-terminal half tau), pSC18 (containing C-terminal half tau), and pSC19 (containing 4-repeats of tau), were generated after introducing *Nde*I/*Bam*HI-cut PCR products into the *Nde*I/*Bam*HI-cut plasmid pAR3040 and transformed into *E. coli* BL21(DE3).

N-Terminal Amino Acid Sequence Determination of Recombinant Human Tau and Its Fragments. Crude protein samples were separated by SDS−PAGE and electroblotted onto a siliconized-glass fiber membrane according to Eckerskorn et al. (*26*). A protein band detected after staining with Coomassie Brilliant Blue was cut out of the membrane, washed in distilled water, and dried, and the N-terminal amino acid sequences were determined using an Applied Biosystems 477A sequencer.

Expression and Purification of Recombinant Human Tau and Its Fragments. Overnight cultures of *E. coli* cells transformed with a parental or recombinant plasmid were diluted 1:10 in fresh medium (NZCYM)(*23*) and grown for 1 h at 37 °C. After adding IPTG to 1 mM and culturing for 1−4 h, the cells were collected by centrifugation. Recombinant tau protein was assessed by resuspending the pellet from 1 mL of culture in 100 μL of sample buffer, boiling for 5 min, and running on a 10% SDS−PAGE gel and then staining with Coomassie Brilliant Blue. Cells containing pSC15 (full-length tau) were treated with lysis buffer (50 mM Tris-HCl, pH 8.0, 1 mM EDTA, 0.1 M NaCl) containing 4 mg of lysozyme, 12.8 mg of sodium deoxycholate, and 20 μL of DNaseI (l mg/mL) per gram of *E. coli* for 1 h at 4 °C, boiled for 10 min, and centrifuged at 27000*g* for 30 min at 4 °C. Tau could be further purified owing to its solubility in 2.5% perchloric acid and insolubility in 25% glycerol (*27*) and by phosphocellulose column chromatography (*6*). Native Alzheimer's PHFs were obtained from Dr. S. Katayama (Mitsubishi Chemical Corp.).

Synthesis of Peptides Corresponding to the C-Tail Region of a Human Tau Isoform. Peptide fragments corresponding to the C-tail region of a human tau, htau 24 isoform (*8*), were synthesized by a solid-phase method (*28*) with a peptide synthesizer (Biosearch Model 9500). As shown in Figure 1, the peptides included C-tail 1 (321−335), C-tail 2 (336−350), C-tail 3 (351−363), C-tail 4 (364−380), C-tail 5 (338−380), C-tail 6 (336−363), C-tail 7 (351−380), and C-tail 8 (326−380). The peptides, each having an N-terminal amino group and a C-terminal carboxyl group, were cleaved from the resin with hydrogen fluoride by the Low-High procedure (*29*) and purified by chromatography on a gel filtration column (Sephadex G-50F or G-25F), ion-exchange column (CM52 or DE52, Whatman), reversed-phase column (Shimpack ODS-PREP(H), Shimadzu), and desalting column (Sephadex G-10). Peptide purity was assessed by TLC, analytical high-pressure chromatography, and amino acid analysis. Peptide sequences were determined by a gas-phase protein sequencer (Applied Biosystems Model 470A). Peptide molecular weight was determined with a FAB mass spectrometer (JEOL HX100).

Preparation of Paired Helical Filaments from Synthetic C-Tail Peptides. Synthetic C-tail peptide fragments were

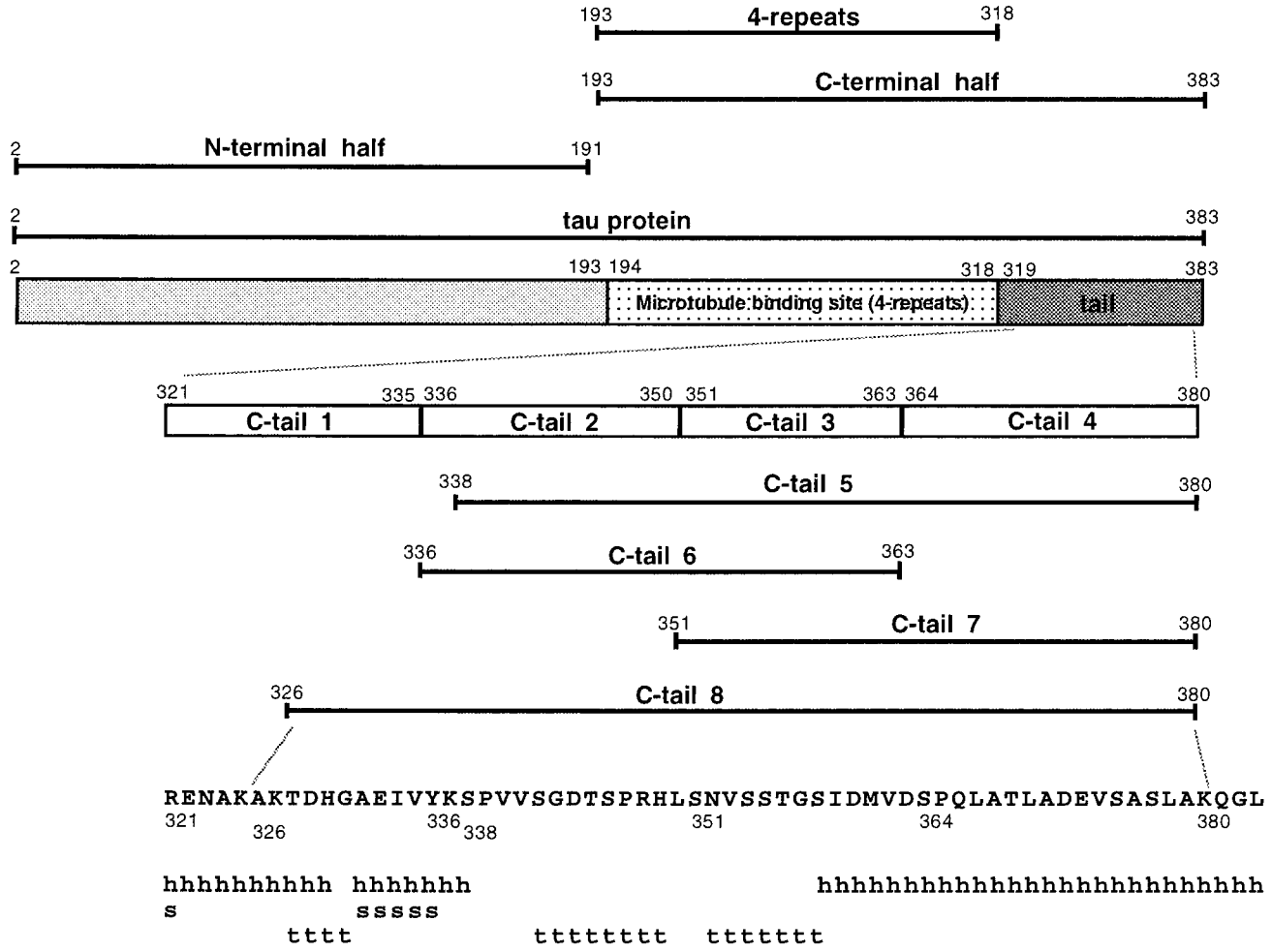

FIGURE 1: Fragments of a human tau isoform, htau 24 (*8*). The residues of the fragments are numbered. The secondary structure of C-tail 8 was predicted by the method of Chou and Fasman (*30*). h, α-helix; s, β-sheet; t, turn. The N-terminus starts from the second amino acid, since the initiating methionine residue is cleaved away in *E. coli* cells.

dissolved in distilled water, 20 mM acetate (pH 4.0), 20 mM MES (pH 6.0), or 20 mM Tris-HCl (pH 7.5) at a final concentration of 0.1−0.3 mM. The solution (200 μL) was placed in an Eppendorf tube (0.5 mL), for incubation at 20 °C.

Transmission Electron Microscopy. For electron microscopy, a drop of sample was placed on a carbon-coated collodion grid, followed by application of 2% uranyl acetate and observation under a JEM 1200EX electron microscope at 80 kV.

CD Measurement. CD spectra were measured at 20 °C on a JASCO J-600 spectropolarimeter equipped with a personal computer and a quartz cell with 1 mm light path. The results were expressed as mean residue ellipticity, [θ]. Temperature was controlled with a thermostatically controlled cell holder. Synthetic C-tail peptides (0.3 mM) were dissolved in distilled water and incubated at 20 °C. Prior to measurement, the sample solution was diluted to 20−30 μM with distilled water to enhance the signal-to-noise ratio, following which no change in CD spectra of the sample could be detected for at least 2 or 3 days. CD spectra of synthetic C-tail peptides were measured in buffer and in buffer containing SDS and TFE, respectively. Sample solutions of the C-tail peptides (30−60 μM) were prepared by diluting stock solutions with 20 mM Tris-HCl (pH 7.5), 20 mM SDS in 20 mM Tris-HCl (pH 7.5) and 40% TFE in 20 mM Tris-HCl (pH 7.5), and CD spectra were measured immediately.

RESULTS

Cloning, Expression, and Purification of Recombinant Human Tau and Its Fragments. Human tau cDNA was amplified by PCR and cloned, and the sequence was determined by dideoxy chain termination. The cloned DNA sequence was identical with previously published human tau clone htau24 cDNA (*8*) except for only a single base (636G→A transition), and there was no change in the corresponding amino acid (Pro). The cloned human tau cDNA was overexpressed in *E. coli* and purified by heat treatment and phosphocellulose column chromatography. The expressed protein was confirmed as true human tau protein based on N-terminal amino acid sequences read as Ala-Glu-Pro-Arg-Gln-Glu-Phe-Glu-Val-Met-Glu-Asp-His-Ala-Gly-Thr-Tyr-Gly, indicating the initiating Met residue to have already been cleaved in *E. coli* cells. Figure 1 illustrates the constructs used in this study. Cloned human tau cDNA served as template DNA for constructing the N-terminal half (1Met to 191Pro), C-terminal half (192Met to 383Leu), and 4-repeat (192Met to 318Leu) sequences, which were also overexpressed in *E. coli* and purified by heat treatment and phosphocellulose column chromatography. Analysis of the N-terminal amino acid sequences indicated deletion of the initiating Met residue. SDS−PAGE of the recombinant

proteins showed full-length tau and its dissected fragments to have molecular weights exceeding those expected from actual mass.

Filamentous Structure Formation from Recombinant Full-Length Tau and Fragments. Study was made to determine whether recombinant tau constructs are capable of self-assembly in aqueous solution. In aqueous solution (water, pH 4.0, and pH 7.5) of recombinant full-length tau after standing at 20 °C, no definite filamentous structures could be found by electron microscopy, as was also the case for aqueous solution (water, pH 4.0, and pH 7.5) of the N-terminal half, 4-repeats, and C-terminal half.

Paired Helical Filament Formation from C-Tail Peptide Fragments. As shown in Figure 1, the C-tail region of full-length tau was first dissected into four segments, as C-tail 1, C-tail 2, C-tail 3, and C-tail 4. The capacity for self-assembly in water, 20 mM acetate (pH 4.0), and 20 mM Tris-HCl (pH 7.5) was examined. Only C-tail 3 formed filamentous structures during prolonged incubation. This tail in water or 20 mM acetate (pH 4) had showed very little linear thin filament formation after incubation at 20 °C for 36 days (data not shown). In 20 mM Tris-HCl (pH 7.5), no formation occurred. Longer C-tail 5, C-tail 6, C-tail 7, and C-tail 8 corresponding to connected segments of C-tail 1 to C-tail 4 (Figure 1) were synthesized and examined for self-assembly and morphology in different aqueous solutions. C-tail 5 in 20 mM acetate (pH 4.0) formed very long SSFs after incubation at 20 °C for 28 days (Figure 2a). SSF is a filament showing a more uniform axial pattern of stain exclusion than PHF under electron microscopic observation. This uniformity may be due to the formation of a strongly twisted helical strand. PHF consists of two filaments wound loosely together. Many separated fine particles mainly 4−20 nm in diameter were formed following dissolution at 20 °C. The separated fine particles gradually assembled near very short single or paired filaments (Figure 2b), which subsequently were slowly transformed into longer paired filaments in parallel. These filaments became loosely twisted and finally turned into long SSFs (Figure 2a). Early in incubation, many fine particles became attached to growing paired filaments but eventually disappeared, all within a period of a month at 20 °C. C-tail 5 formed short paired filaments in parallel in water after incubation at 20 °C for 63 days. C-tail 5 in 20 mM MES (pH 6) and 20 mM Tris-HCl (pH 7.5) showed no filaments under the same conditions. C-tail 6 produce no filamentous structures in 20 mM acetate (pH 4.0) or water.

C-tail 7 formed several thin filaments in parallel in water after incubation at 20 °C for 5.5 h (Figure 2c). Similar filamentous structures were formed in 20 mM acetate (pH 4.0) but were shorter than in water. No filamentous structures could be seen in 20 mM MES (pH 6.0) or 20 mM Tris-HCl (pH 7.5).

As shown in Figure 3, C-tail 8 containing most of the tail region of tau protein produced many parallel paired filaments in water and 20 mM acetate (pH 4.0) after incubation at 20 °C. Single and paired filaments were 5−6 and 13 nm in diameter, respectively. At the start of formation, many fine particles could be seen attached to the filaments (Figure 3a), but these gradually disappeared and were replaced by many parallel paired filaments (Figure 3b). Most of the fine particles were completely converted into parallel paired filaments after 26 days (Figure 3c). Essentially the same was noted for C-tail 5. Longer incubation time led to very closely assembled parallel paired filament formation (Figure 3d). This formation from C-tail 8 was noted to occur at pH 3−4 and below, where, only shorter pairs were evident (data not shown). At pH 5−5.5, several parallel paired filaments became loosely twisted (data not shown). At pH 6−7.5, only a fine particle aggregate could be seen.

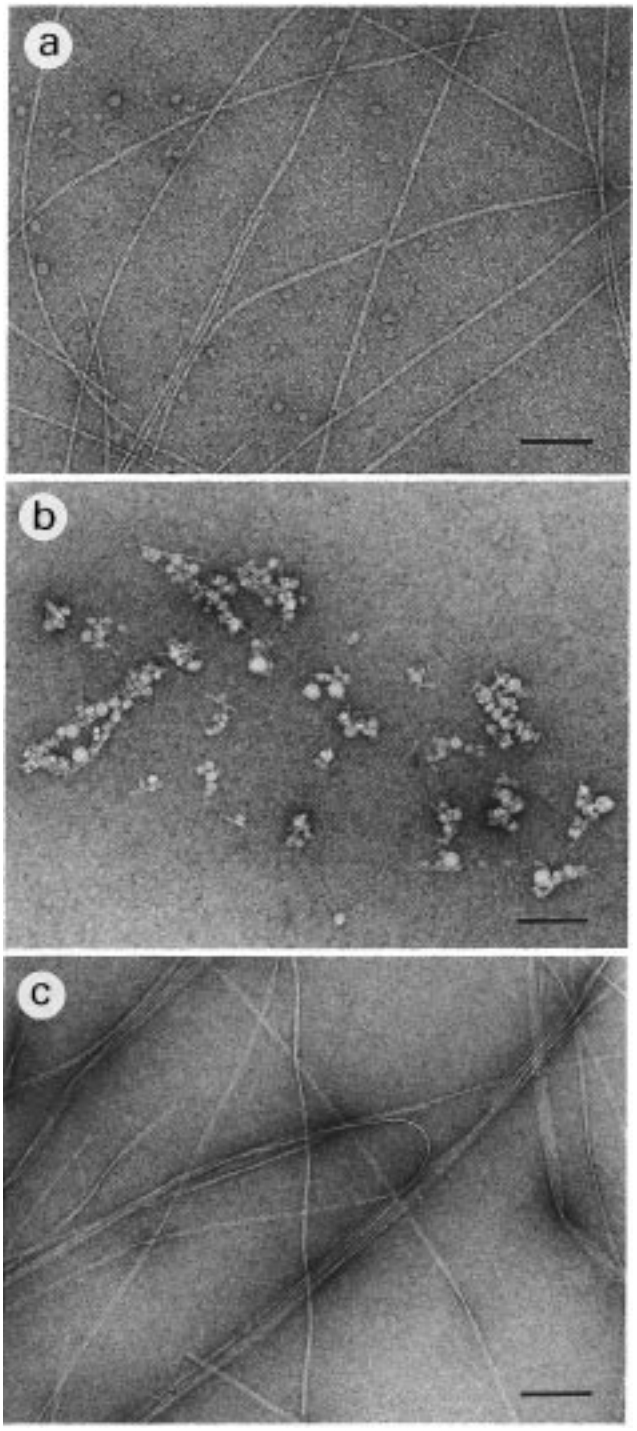

FIGURE 2: Electron micrograph of filamentous structures formed from C-tail 5 and C-tail 7. (a) C-tail 5 (0.146 mM) in 20 mM acetate buffer (pH 4.0) was incubated at 20 °C for 28 days. (b) C-tail 5 (0.146 mM) in 20 mM acetate buffer (pH 4.0) was incubated at 20 °C for 7 days. (c) C-tail 7 (0.3 mM) in water was incubated at 20 °C for 5.5 h. Scale bars represent 100 nm.

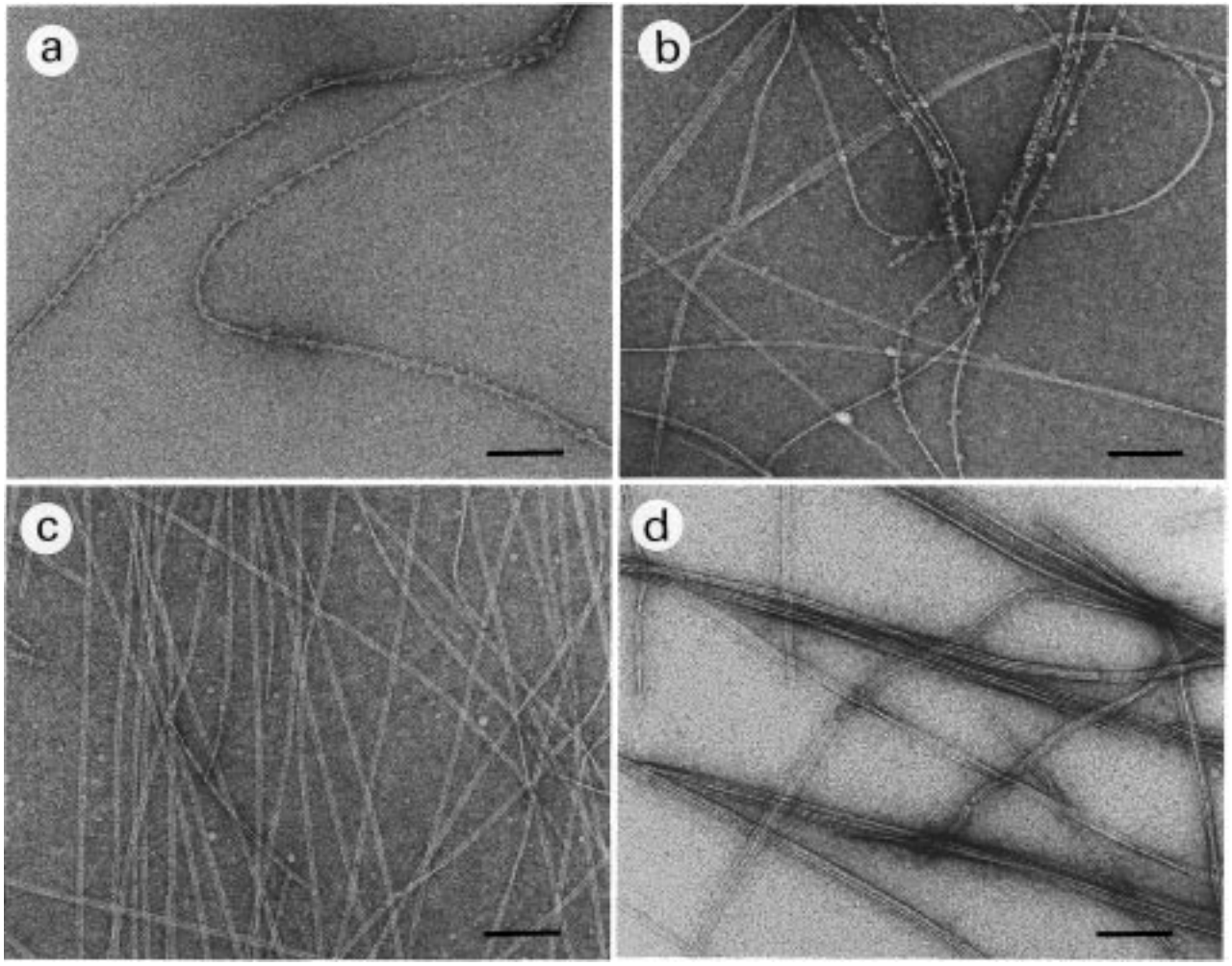

FIGURE 3: Electron micrograph of different types of filamentous structures formed from C-tail 8. C-tail 8 (0.088 mM) in water was incubated at 20 °C for 9 days (a), 18 days (b), 26 days (c), and 29 days (d). All scale bars represent 100 nm.

C-Tail Peptide Fragment Conformation in Aqueous Solution. The CD spectra of C-tail peptide fragments were measured immediately following dissolution in water, 20 mM acetate (pH 4.0), 20 mM Tris-HCl (pH 7.5), 20 mM Tris-HCl (pH 7.5) containing 20 mM SDS, and 20 mM Tris-HCl (pH 7.5) containing 40% TFE. The CD spectra of the C-tail peptide fragments (C-tails 1−8) in water or buffer alone showed all peptide fragments to have unordered structures. C-tail 4, C-tail 5, C-tail 7, and C-tail 8 assumed α-helical structures in 20 mM SDS and 40% TFE (Figure 4), but C-tail 1, C-tail 2, C-tail 3, and C-tail 6 remained essentially random under the same conditions (data not shown). C-tail 4, C-tail 5, C-tail 7, and C-tail 8 in SDS and TFE solution were examined for their ability to aggregate, based on molar ellipticity in 20 mM SDS and 40% TFE. Between 5 and 120 μM, the molar ellipticity at 220 nm changed less than 5%, indicating essentially no aggregation.

C-Tail 7 and C-Tail 8 Conformation in Water. Both tail CD spectra were noted following incubation at 20 °C in water (Figure 5). The CD spectrum of C-tail 7 measured immediately after dissolution showed a negative maximum value below 200 nm, indicating a random coil structure to be predominant (Figure 5a). Rapid change in the CD spectrum was evident following incubation at 20 °C. The negative Cotton effect at 218 nm became remarkably stronger, indicating the formation of the β-sheet structure assumption (Figure 5a). $[\theta]_{218\ nm}$ after incubation for 8 h was 2.5 times that immediately following dissolution. A gradual change in the CD spectrum after a day was noted for C-tail 7 in aqueous solution. Strikingly greater negative Cotton effect was noted with two peaks at 208 and 220 nm, indicating α-helical structure formation. CD spectra at different times of incubation showed no isodichroic point. An aqueous solution of C-tail 7 would thus appear to cause a three-state transition, as random coil → β-sheet → α-helix.

The CD spectrum of C-tail 8 in water measured immediately after dissolution showed a negative peak at 198 nm, indicating C-tail 8 predominantly to take on a random coil structure (Figure 5b). No gradual change in the CD spectrum was noted after incubation at 20 °C. A negative peak at 198 nm very slowly shifted to 218 nm, indicating predominantly a β-sheet structure for the peptide. CD spectra at different times of incubation showed isodichroic points at 206 nm, and thus a two-state transition. The intensity of the negative peak at 218 nm was easily altered by the presence of parallel paired filaments. A solution containing many such filaments showed a strong negative peak at 218 nm. Figure 6a shows the time course of ellipticity at 218 nm. This parameter at 0.088 mM did not change for 22 days but thereafter gradually increased to a maximum in 29 days. For β-sheet structure formation, there was thus a lag time of 22 days; formation proceeded logarithmically, finally

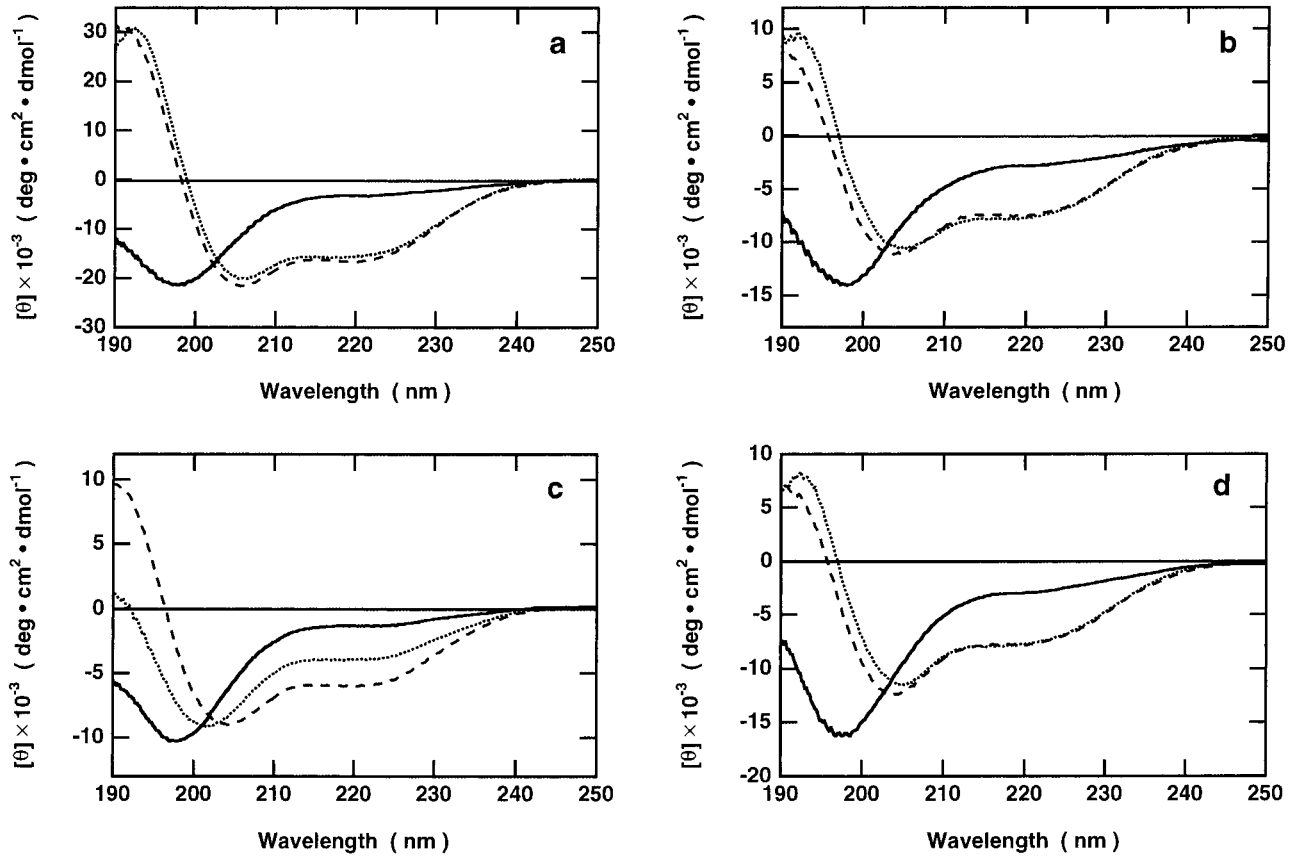

FIGURE 4: CD spectra of C-tail 4 (a), C-tail 5 (b), C-tail 7 (c), and C-tail 8 (d) in different solutions. CD spectra were measured in 20 mM Tris-HCl (pH 7.5) (—), 20 mM Tris-HCl (pH 7.5) containing 20 mM SDS (···), and 20 mM Tris-HCl (pH 7.5) containing 40% TFE (---) at 20 °C.

reaching a plateau in 29 days. That paired filaments subsequently accelerated the formation of this structure appears to reflect the occurrence of these events. Figure 6a,b indicates higher concentration of C-tail 8 and higher incubation temperature to lessen the lag time of transformation. At 60 °C, C-tail 8 rapidly assumed the β-sheet structure though there was considerable precipitation of this tail after incubation for 3 days. The optimum pH for β-sheet structure formation was 3−4, the same as that of paired filaments.

Figure 6c shows the effects of preformed paired filament on the rate of transition from a random coil to β-sheet structure. The increase in negative ellipticity at 218 nm was significantly accelerated by a small number of preformed paired filaments. The structural change was proportional to added preformed paired filaments, and thus was mediated by a mechanism in which paired filaments autocatalytically accelerate filament formation. That is, preformed paired filaments served as a template for subsequent formation. The formation of a small number of paired filaments leads to PHF formation.

Interaction of Full-Length Tau with C-Tails 5, 7, and 8. Neither full-length tau nor C-tail produced any filaments in MES (pH 6.0), but did so through interactions with each other in this buffer. An equimolar mixture of full-length tau and C-tail 5 or C-tail 7 produced loosely twisted paired filaments in MES (pH 6) following prolonged incubation (Figure 7a,b). Such a mixture of full-length tau and C-tail 8 formed tightly twisted paired filaments resembling SSFs in MES (pH 6.0) after incubation for 154 days (Figure 7c). Paired filament formation thus appears to occur slowly in the mixture at pH 6.0. The addition of preformed paired filaments to the mixture considerably accelerated the formation of tightly twisted paired filaments.

DISCUSSION

PHFs are composed of the microtubule-associated protein tau, in a hyperphosphorylated state. The hyperphosphorylation of tau rendered it incapable of binding to microtubules. The abnormal phosphorylation of tau was previously considered a prerequisite for self-assembly into PHFs (*7*). Extensive conformational change occurs when tau protein is converted to PHF. Some amino and carboxy termini of tau are cleaved in extracellular tangles, indicating the core of PHF to possibly be comprised of three to four tandem repeat regions of tau which normally functions in the microtubule-binding domain (*31*). Only shortened 3-repeat tau fragments have been shown to assemble in paired helical-like filaments *in vitro* (*19*).

For further clarification of the structural features of tau required for PHF formation *in vitro*, a method for producing PHFs *in vitro* should be established. A recombinant isoform (htau 24) of human tau and its fragments, the N-terminal half, C-terminal half, and 4-repeats expressed in *E. coli*, were prepared and examined for self-assembly *in vitro*. No PHF formation from recombinant full-length tau or fragments in normal aqueous solution could be found. Tau isolated from brain tissue self-assembles into fibrous structures (*15, 16*). PHF-like structures have been observed from recombinant human tau with 4-repeats corresponding to the 441 amino acid isoform (htau40) expressed in *E. coli* (*32*).

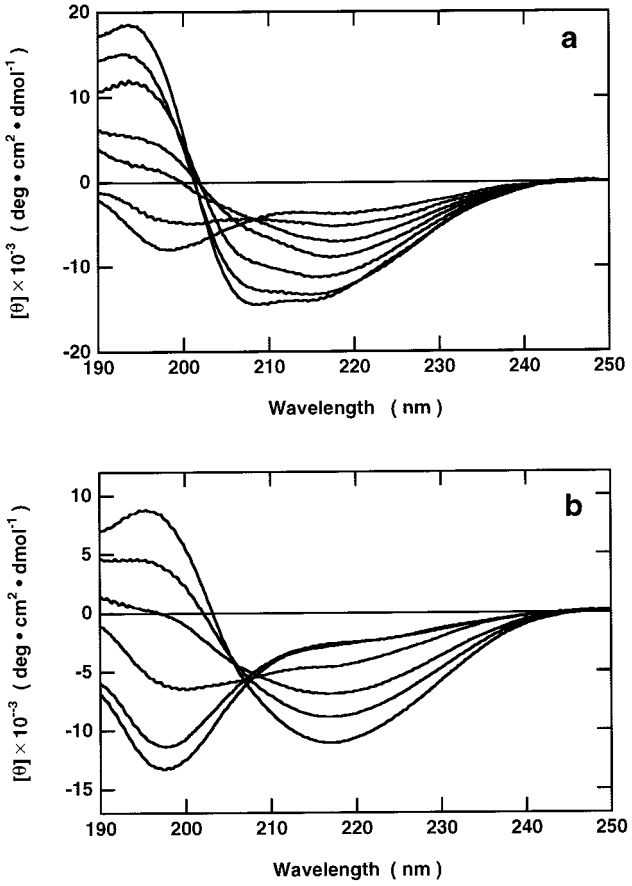

FIGURE 5: CD spectra of C-tail 7 and C-tail 8 in water. (a) Spectra of C-tail 7 (0.3 mM) were obtained immediately following dissolution after incubation for 0 h, 2 h, 5.5 h, 8 h, 1 day, 2 days, and 3 days at 20 °C, reading downward at 215 nm. (b) Spectra of C-tail 8 (0.088 mM) were obtained after incubation for 18, 21, 24, 26, 28, and 29 days at 20 °C, reading downward at 218 nm.

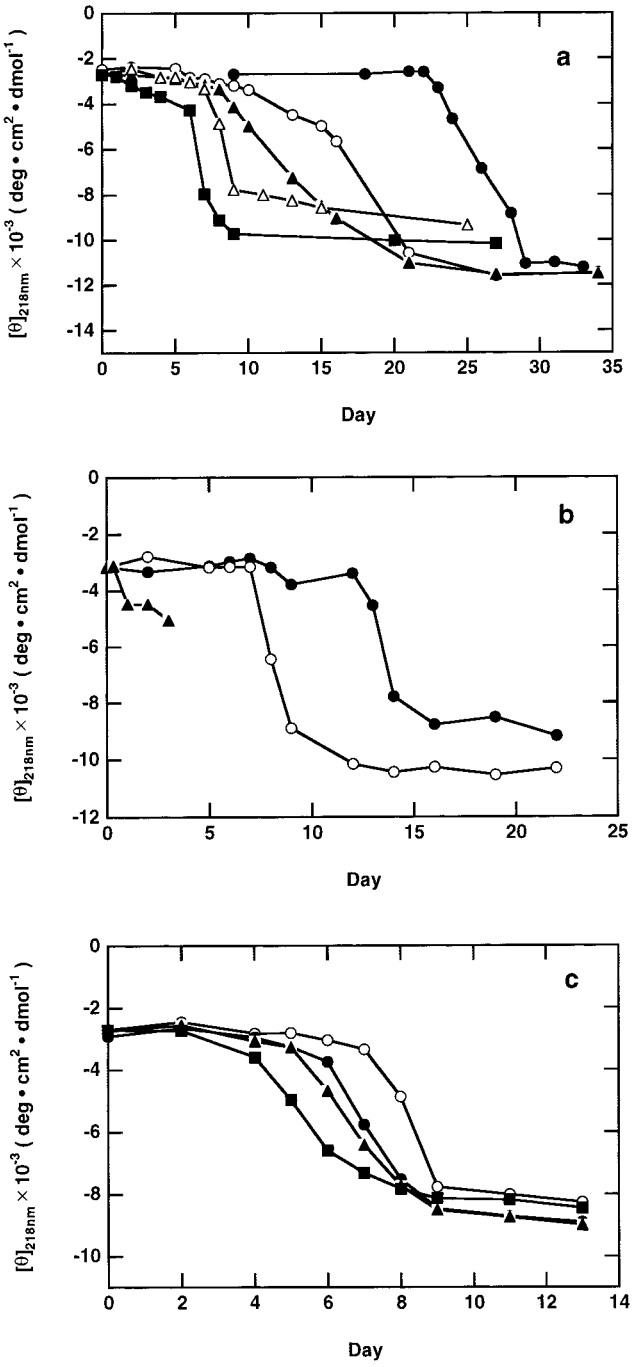

FIGURE 6: (a) Time course of β-sheet structure formation from C-tail 8 in water at 20 °C. The formation of β-sheet structures was monitored as the increase in negative mean residue ellipticity at 218 nm. Concentration of C-tail 8: 0.088 (●), 0.1 (○), 0.15 (▲), 0.2 (△), and 0.35 mM (■). (b) Effects of temperature on the formation of β-sheet structures form C-tail 8. β-Sheet structure formation was monitored as the increase in negative mean residue ellipticity at 218 nm. Aqueous solution (0.3 mM) of C-tail 8 in water was incubated at 20 °C (●), 37 °C (○), and 60 °C (▲), respectively. The CD spectrum after incubation for 4 days at 60 °C could not be measured owing to the large amount of precipitate in solution. (c) Rate enhancement of β-sheet structure formation by preformed aggregate. The formation was monitored as the increase in negative mean residue ellipticity at 218 nm. Aqueous solution (0.2 mM) of C-tail 8 in water was incubated at 20 °C with preformed aggregate at 0 μM (○), 1 μM (●), 2 μM (▲), and 4 μM (■), respectively.

Nonphosphorylated recombinant tau and hyperphosphorylated tau have recently been shown to form PHFs in the presence of sulfated glycosaminoglycans such as heparin and heparan sulfate (*33*). Such structures have been prepared under certain conditions such as dialysis of the urea-soluble fraction of tau of porcine brain and its microtubules, spraying of glycerol solution of tau, vapor diffusion in hanging drops in the protein crystallization, and the presence of sulfated glycosaminoglycans. These conditions differ from those of this study in which aqueous solution containing tau was made to stand without disturbance over a long period at 20 °C. PHF-like structure formation would thus appear to occur only under special conditions. Vapor diffusion in hanging drops increases the concentration of tau. A few short rod structures were noted to form at 60 °C (data not shown). An aqueous solution of recombinant full-length tau showed a negative Cotton effect at 194 nm, thus indicating a random structure. This effect at 194 nm decreased with rise in temperature from 10 to 70 °C. Thus, with increasing temperature, the random structure disappears and is replaced with a more ordered secondary structure (*34*). This situation has also been noted for elastin. Below 20 °C, elastin extension occurs, and at 37 °C, elastin is coacervated to form filaments (*35*).

C-tail fragments of tau, C-tail 5, C-tail 7, and C-tail 8, formed paired filaments in acidic aqueous solution. Hydrophobic amino acids of these C-tail fragments were present at 35% (C-tail 5), 40% (C-tail 7), and 35% (C-tail 8), respectively, these values exceeding those for htau24 (24%).

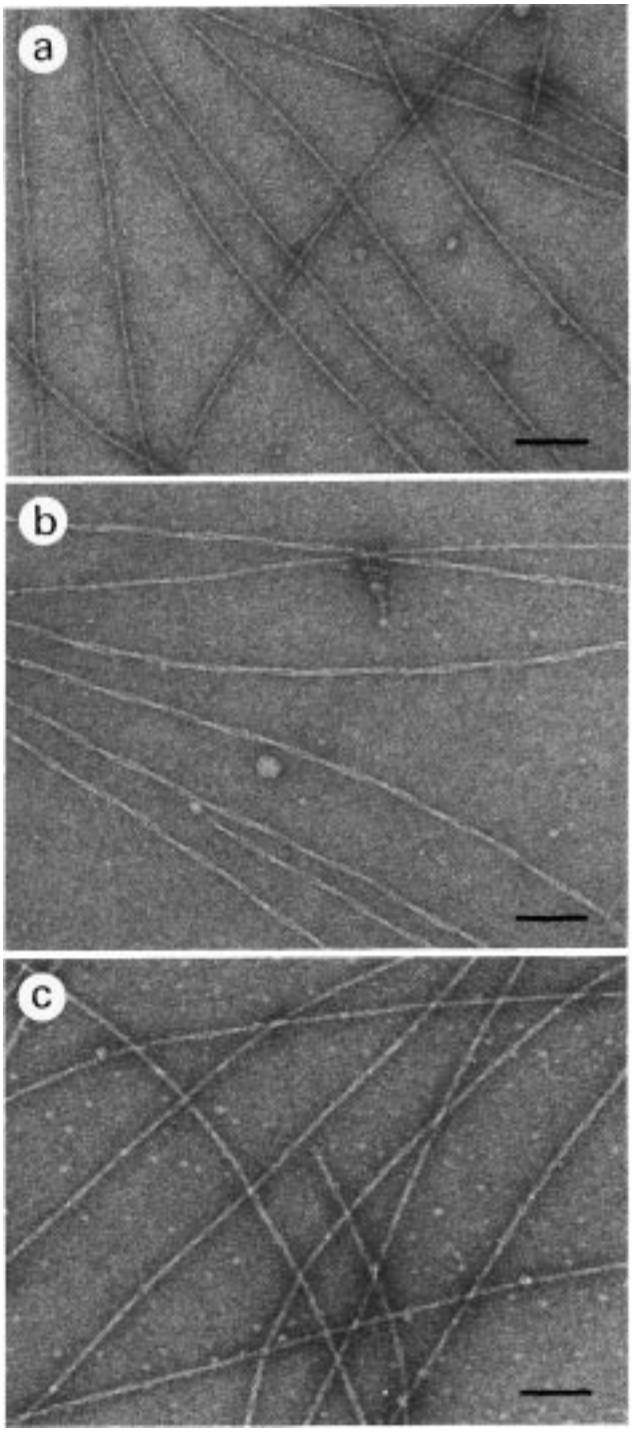

FIGURE 7: Electron micrograph of filaments formed from a mixture of recombinant full-length tau and C-tails. A mixture of 0.124 mM recombinant full-length tau and 0.146 mM C-tails 5 (a), 7 (b), and 8 (c) in MES buffer (pH 6.0) was incubated at 20 °C for 71 days, 54 days, and 154 days, respectively. All scale bars represent 100 nm.

This higher hydrophobicity may be an indication of paired filament formation. Hydrophobic amino acids were most abundant in C-tail 7 (40%). The rates of paired filament formation under identical conditions followed the order: C-tail 7 > C-tail 8 > C-tail 5. Paired filament formation from C-tail 7 was observed after 1 day but for C-tail 8 after 21 days and for C-tail 5 28 days. The rapid change in morphology of C-tail 7 was supported by its CD spectrum. Acidic solution of C-tail 7 showed rapid change in its CD

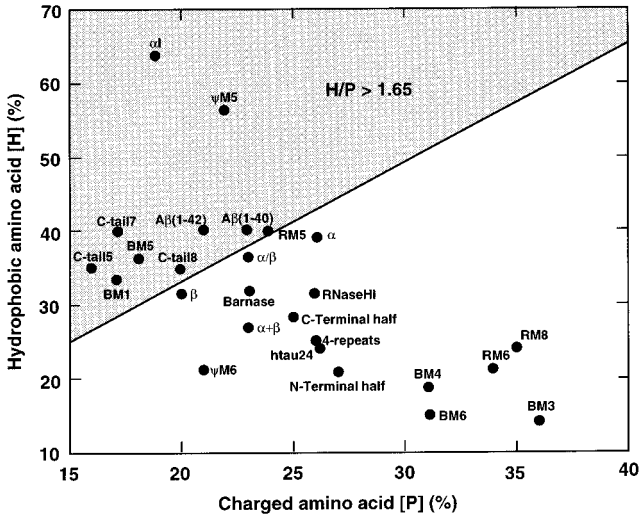

FIGURE 8: Mapping percentages of amino acid compositions of different proteins and peptides. Ordinates and abscissas represent the content of hydrophobic amino acids (Ala, Ileu, Leu, Met, Phe, and Val) and charged amino acids (Asp, Glu, Lys, and Arg). BM1, BM3, BM4, BM5, and BM6, residues 1−24, 52−73, 73−88, 88−98, and 99−110 corresponding to modules of barnase (*37*); RM5, RM6, RM8, residues 53−77, 78−106, and 120−136 corresponding to modules of RNase HI (*39*); ψM5, ψM6, and αI, residues 43−69, 66−93, and 43−58 corresponding to secondary structures of RNase HI (*39*); Aβ(1−40) and Aβ(1−42), residues 672−711 and 672−713 of amyloid β precursor protein (40); α, β, α + β, and α/β, norms of amino acid composition of 4-folding types of natural proteins (*41*).

spectrum after incubation at 20 °C. The CD spectrum measured after several hours showed a negative maximum at 218 nm, indicating predominantly the β-sheet structure (Figure 5a).

Figure 8 presents the amino acid compositions of tau fragments, Aβ peptides, and module fragments of barnase and RNase HI. Filament-forming peptide fragments were situated in an area where *H*/*P* was 1.65 or above. *H*/*P* is the ratio of the content of hydrophobic amino acids (*H*) to charged amino acids (*P*). htau24 and its C-terminal half, N-terminal half, and 4-repeats were situated at a site with *H*/*P* below 1.65. A module is a compact structural unit in a globular protein or domain (*36*), and its boundaries are determined primarily by intron positions of genes that encode proteins. Modules and/or their assembly may have roles in primitive proteins (*37*). The assembly of disconnected modules in aqueous solution was studied for confirmation of this point. Module 1 (1−24, 24-mer) fragment of barnase formed helical filaments in aqueous solution (*38*). Peptide fragments such as module 5 (53−77, 25-mer), pseudomodule 5 (43−69, 27-mer), and αI (43−58, 16-mer) of RNase HI (*39*) also produced filaments in acidic solutions.[2] Aβ (1−40) and Aβ (1−42) corresponding to residues 672−711 and 672−713 of amyloid β precursor protein formed amyloid fibrils *in vitro* (*40*).

Secondary structure prediction based on the alignment of htau24 sequence (*30*) indicated two putative helical regions in the C-tail (Figure 1). C-tail 5 and C-tail 7 each contained a putative helical region and C-tail 8, two putative helical regions. These three C-tails all possessed helical structures in lipophilic solution containing TFE and SDS and random

[2] H. Yanagawa et al., submitted for publication.

coil structures in aqueous solutions. C-tails 5 and 7 assumed β-sheet structures in an acidic solution after incubation at 20 °C. Figure 8 indicates most filament-forming peptides have helical structures in lipophilic solutions containing TFE and SDS. Such peptides were module 1 of barnase, module 5, and pseudomodule 5 of RNase HI and Aβ peptides.

C-tail 5 and C-tail 7 interacted with full-length recombinant tau (htau24) to form loosely twisted paired filaments resembling PHFs, and C-tail 8 interacted with full-length recombinant tau to form tightly twisted paired filaments similar to SSFs in aqueous solution. Interactions between full-length tau and its C-tails may thus possibly lead to neurofibrillary lesion formation in Alzheimer's disease. These lesions consist of PHFs and SSFs containing hyperphosphorylated tau protein unable to bind to microtubules. Under physiological conditions, phosphorylation-independent interactions between full-length recombinant tau and C-tail 8 lead to the formation of SSFs. Four independent tau peptides located in the carboxyl third of tau were found in the protease digest of PHF from Alzheimer's disease brain (*42*). C-tail regions derived from full-length tau by digestion with protease may thus be tightly bound to full-length tau to form PHF *in vivo*. C-tail peptide fragments may serve as templates for subsequent PHF formation *in vivo*. At 5 °C, filament formation from the N-terminal module of barnase was previously shown to proceed slowly (*38*). For the C-tail region of tau, the most remarkable feature of the negative ellipticity at 218 nm was the considerably long lag phase (Figure 6a,b), characteristic of separate initiation reactions, with kinetics differing from those of propagation. The formation of oligomeric nuclei as initiation sites may be the reason for this. To confirm this point, a small number of seeds of preformed filaments was added to a fresh C-tail 8 solution, resulting in significantly increased negative ellipticity at 218 nm. The polymerization of C-tail peptides of tau into filaments was similar to that of prion from the viewpoints of conformational change and self-propagation. The proteins and peptides causing conformational change and self-propagation *in vitro* were thus termed "*in vitro* prions". The *in vitro* prion includes C-tail 8 (326−380, 55-mer) of tau, module 1 (1−24, 24-mer) of barnase (*38*), and pseudomodule 5 (43−69, 27-mer) of *E. coli* RNase HI.[2]

Two models for the conformational conversion of a prion have been proposed: a heterodimer model and a seeding model (*43*). In the former, conformational change is thermodynamically controlled and catalyzed by $PrP^{Sc}-PrP^{C}$ heterodimer formation. In the latter, seed formation occurs in accordance with a nucleation-dependent polymerization mechanism, kinetically controlled and extremely slow; once a seed is present, monomer addition ensues rapidly. The present data are consistent with a necleation-dependent polymerization mechanism having two distinctive features. Nucleation-dependent polymerization shows a lag time before filaments are detectable (Figure 6a). Lag time was strongly dependent on C-tail peptide concentration. During lag time, nuclei could be found in trace amounts. Many fine particles were observed at the initial stage of filamentous structure formation by electron microscopy (Figure 2b). These particles gradually decreased with increase in the number of filaments and appeared to indicate nuclear aggregation. In addition to lag time, seeding was also noted (Figure 6c). Nucleation determines the rate of filament formation at low supersaturation. The addition of seeds thus immediately brings about polymerization. C-tail peptide fragments may initiate PHF formation *in vivo* via a nucleation-dependent polymerization mechanism. Replication of C-tails may possibly be due to proteolytic fragmentation of PHF.

ACKNOWLEDGMENT

We thank Prof. Y. Sakaki (University of Tokyo) for providing human brain cDNA library, Dr. S. Katayama (Mitsubishi Chemical Corp.) for providing native Alzheimer's PHFs, and Dr. A. Ohmori at this institute for assistance in amino acid sequence analysis.

REFERENCES

1. Goldstein, L. S. B., Laymon, R. A., and Mcintosh, J. R. (1986) *J. Cell Biol. 102*, 2076−2087.
2. Gard, D. L., and Kirschner, M. W. (1987) *J. Cell Biol. 105*, 2203−2215.
3. Binder, L. I., Furankfurter, A., and Rebhun, L. I. (1985) *J. Cell Biol. 101*, 1371−1378.
4. Garner, C. C., Tucker, R. P., and Matus, A. (1988) *Nature 336*, 674−677.
5. Kosik, K. S., and Finch, E. A. (1987) *J. Neurosci. 7*, 3142−3153.
6. Cleveland, D. W., Hwo, S.-Y., and Kirschner, M. W. (1977) *J. Mol. Biol. 116*, 207−225.
7. Goedert, M., Wischik, C. M., Crowther, R. A., Walker, J. E., and Klug, A. (1988) *Proc. Natl. Acad. Sci. U.S.A. 85*, 4051−4055.
8. Goedert, M., Spillantini, M. G., Potier, M. C., Ulrich, J., and Crowther, R. A. (1989) *EMBO J. 8*, 392−399.
9. Himmler, A. (1989) *Mol. Cell. Biol.* 9, 1389−1396.
10. Wischik, C. W., Novak, M., Edwards, P. C., Klug, A., Tichelaar, W., and Crowther, R. A. (1988) *Proc. Natl. Acad. Sci. U.S.A. 85*, 4884−4888.
11. Khatoon, S., Grundke-Iqbal, I., and Iqbal, K. (1992) *J. Neurochem. 59*, 750−753.
12. Jakes, R., Novak, M., Davison, M., and Wischik, C. M. (1991) *EMBO J. 10*, 2725−2729.
13. Wischik, C. W., Crowther, R. A., Stewart, M., and Roth, M. (1985) *J. Cell Biol. 100*, 1905−1912.
14. Montejo de Garcini, E., Serrano, L., and Avila, J. (1986) *Biochem. Biophys. Res. Commun. 141*, 790−796.
15. Montejo de Garcini, E., and Avila, J. (1987) *J. Biochem. 102*, 1415−1421.
16. Lichtenberg-Kraag, B., and Mandelknow, E.-M. (1990) *J. Struct. Biol. 105*, 46−53.
17. Ksiezak-Reding, H., and Yen, S.-H. (1991) *Neuron 6*, 717−728.
18. Andreadis, A., Brown, W. M., and Kosik, K. S. (1992) *Biochemistry 31*, 10626−10633.
19. Wille, H., Drewes, G., Biernat, J., Mandelkow, E. M., and Mandelkow, E. (1992) *J. Cell Biol. 118*, 573−584.
20. Goedert, M., and Jakes, R. (1990) *EMBO J. 9*, 4225−4230.
21. Caputo, C. B., Sygowski, L. A., Scott, C. W., and Sobel, I. R. E. (1992) *Brain Res. 597*, 227−232.
22. Crowther, R. A., Olesen, O. F., Jakes, R., and Goedert, M. (1992) *FEBS Lett. 309*, 199−202.
23. Sambrook, J., Fritsch, E. F., and Maniatis, T. (1989) *Molecular Cloning: A laboratory Manual*, Cold Spring Harbor Laboratory Press, Cold Spring Harbor, NY.
24. Sanger, F. W., Nicklen, S., and Coulson, A. R. (1977) *Proc. Natl. Acad. Sci. U.S.A. 74*, 5463−5467.
25. Rosenberg, A. H., Barbara, N. L., Chui, D.-S., Lin, S.-W., Dunn, J. J., and Studier, F. W. (1987) *Gene 56*, 125−135.
26. Eckerskorn, C., Mewes, W., Goretzki, H., and Lottspeich, F. (1988) *Eur. J. Biochem. 176*, 509−519.
27. Lindwall, G., and Cole, R. D. (1984) *J. Biol. Chem. 259*, 12241−12245.
28. Merrifield, R. B. (1963) *J. Am. Chem. Soc. 85*, 2149−2154.

29. Tam, J. P., Heath, W. F., and Merrifield, R. B. (1983) *J. Am. Chem. Soc. 105*, 6442−6455.
30. Chou, P. Y., and Fasman, G. D. (1979) *Biophys. J. 26*, 367−384.
31. Goedert, M. (1993) *Trends Neurosci. 16*, 460−465.
32. Crowther, R. A., Olesen, O. F., Smith, M. J., and Goedert, M. (1994) *FEBS Lett. 337*, 135−138.
33. Goedert, M., Jakes, R., Spillantini, M. G., Hasegawa, M., Smith, M. J., and Crowther, R. A. (1996) *Nature 383*, 550−553.
34. Ruben, G. C., Iqbal, K., Grundke-Iqbal, I., Wisniewski, H. M., Ciardelli, T. L., and Johnson, J. E., Jr. (1991) *J. Biol. Chem. 266*, 22019−22027.
35. Cox, B. A., Starcher, B. C., and Urry D. W. (1973) *Biochim. Biophys. Acta 317*, 209−213.
36. Go, M. (1983) *Proc. Natl. Acad. Sci. U.S.A. 80*, 1964−1968.
37. Yanagawa, H., Yoshida, K., Torigoe, C., Park, J.-S., Sato, K., Shirai, T., and Go, M. (1993) *J. Biol. Chem. 268*, 5861−5865.
38. Yoshida, K., Shibata, T., Masai, J., Sato, K., Noguti, T., Go, M., and Yanagawa, H. (1993) *Biochemistry 32*, 2162−2166.
39. Doi, N., Itaya, M., Yomo, T., Tokura, S., and Yanagawa, H. (1997) *FEBS Lett. 402*, 177−180.
40. Selkoe, D. J. (1994) *Annu. Rev. Cell Biol. 10*, 373−403.
41. Chou, K.-C. (1995) *FEBS Letts 363*, 127−131.
42. Kondo, J., Honda, T., Mori, H., Hamada, Y., Miura, R., Ogawara, M., and Ihara, Y. (1988) *Neuron 1*, 827−834.
43. Weissman, C. (1996) *FEBS Lett. 389*, 3−11.

BI9724265